PCaDA statement of methods

Andrea Collina, Stefano Bruni, Alan Facchinetti* and Andrea Zuin

Dipartimento di Meccanica, Politecnico di Milano, Via La Masa 1, 20156 Milano, Italy

(*Received 18 May 2014; accepted 22 August 2014*)

1. Introduction

This paper provides an overview of the simulation code PCaDA (Pantograph–Catenary Dynamic Analysis) for the numerical simulation of pantograph–catenary interaction. Research work on this subject at Politecnico di Milano started at the end of the 1980s with the PhD thesis by A. Collina, which resulted in the first version of the simulation software. During the design phase of the Italian high-speed railway network, early versions of PCaDA were used to support the design of the catenaries for 25 kV AC and for 3 kV DC. As part of this process, extensive measurement campaigns were performed, against which the software was validated.

More recently, the modelling and simulation capabilities of PCaDA were extended to incorporate several advanced features, mostly meant to widen the frequency range covered by the simulation, as detailed in Section 3. The software in its present form was further validated against line measurements performed on French and German high-speed catenaries and on a Swedish catenary for conventional speed. It has been used to design an improved 25 kV AC catenary for 360 km/h speed in Italy and to validate the design of several catenaries across the world, including conductor bar catenaries and other types of special catenaries.

The simulation method implemented in PCaDA is based on a finite element (FE) model of the catenary and a lumped parameter model of the pantograph. The catenary model is defined using tensioned Euler–Bernoulli beams for the messenger and contact wire and a lumped model or beam element model for the suspension and the steady arm. Different types of catenaries can be modelled, including simple catenaries, stitched wire, and conductor bar catenaries. Overlap sections can also be considered.

*Corresponding author. Email: alan.facchinetti@polimi.it

For the droppers, different types of nonlinear models are available, including the possibility to use the force–deformation characteristic curve of the dropper as measured in a laboratory experiment. Research work is ongoing to introduce further refined models of the droppers, capable of reproducing not only the quasi-static, but also the dynamic behaviour of the droppers as measured in the laboratory.

The pantograph is modelled as a lumped parameter system, but the flexibility of the collec-tors can be accounted for by using mode superposition. The contact between the pantograph and the catenary is modelled using the penalty method.[2]

The code is fully 3D and allows to consider the effect of excitation/disturbance sources such as wind effects and the motion of the pantograph base frame resulting from the running behaviour of the railway vehicle.

The simulation code is written in FORTRAN. A graphic user interface was developed in MATLAB allowing the automated generation of the inputs for the simulation, the management of databases for catenaries and pantographs, and the post-processing of the results. Specific post-processors were also developed to analyse wear on the contact wire and on the contact strips in the pantograph head. The databases allow to store in ascii files the mechanical properties and the geometry of the following elements: pantographs, catenary suspensions, contact wires, droppers, messenger wires, conductor bars, and the specific elements installed in a conductor bar catenary (e.g. section insulators and expansion joints).

2. Methods as applied in the benchmark

A detailed description of the PCaDA's features used in the benchmark is provided in this section, together with the description of how the models were set-up.

2.1. *Catenary model*

The catenary model is defined according to the finite element method and consists of 30 identical spans. Transitions are not modelled. The contact wire and the messenger wire are schematised using 2D or 3D Euler–Bernoulli tensioned beam elements,[1] depending on the considered simulation case. Figure 1 shows a 3D sketch of the catenary, whereas Table 1 shows the main characteristics for the contact wire and for the messenger wire. The complete set of input data for the catenary model is reported in the appendix of the paper summarising the benchmark results. Table 1 also reports the numbers of finite elements per span adopted for the catenary model, chosen in order to keep the length of the element smaller than 1 m, and the resulting lowest natural frequencies of the finite elements. As can be observed, these natural frequencies fall significantly above the frequency range of interest (0–20 Hz) so that the single finite element can be considered to preserve a quasi-static behaviour, as prescribed by the theory of finite elements.

The droppers are also modelled as Euler–Bernoulli tensioned beam elements (one element per dropper), except for the axial dynamics that is represented by considering the nonlinear force–displacement relationship in order to take dropper slackening into account. In particular, a bi-linear behaviour is considered in the benchmark, with linear stiffness when the dropper is stretched and zero force when the dropper is compressed.

The messenger wire suspensions at the masts are represented using a lumped model consisting of a set of vertical and longitudinal springs and dampers (cf. Table 2). In the 3D model of the catenary, the steady arm is modelled using four tensioned beams with a spheri-cal hinge at the mast, whereas in the 2D catenary model a simplified steady arm model is used,

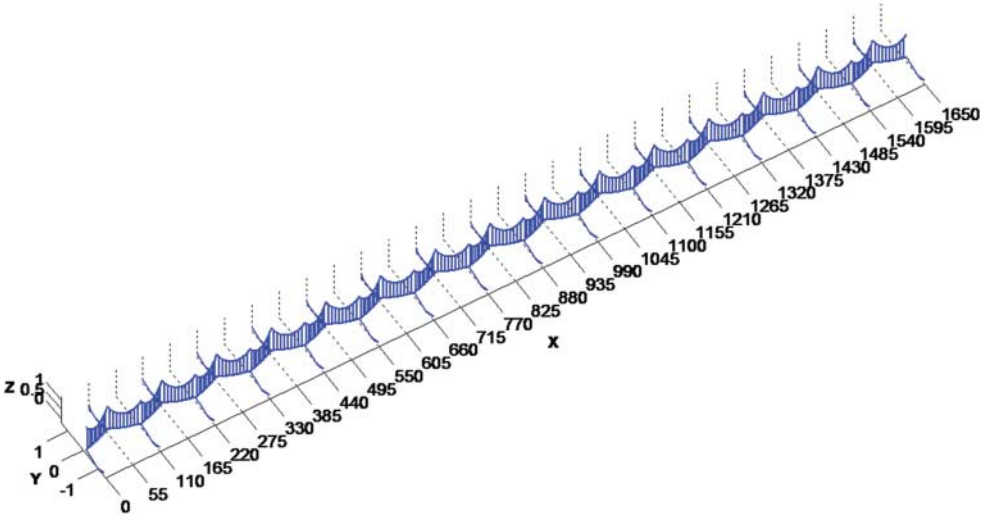

Figure 1. 3D sketch of the catenary.

Table 1. Contact wire and messenger wire main data.

	Section (mm^2)	Mass/unit length (kg/m)	Tension (kN)	Number of beams/span	Element lowest frequency (Hz)
Contact wire	150	1.35	22	58	69.7
Messenger wire	120	1.08	16	58	67.4

Table 2. Catenary suspension and steady arm data.

2D/3D catenary	Messenger wire suspension vertical stiffness (kN/m)	500
	Messenger wire suspension vertical damping (kNs/m)	1.0
	Messenger wire suspension longitudinal stiffness (kN/m)	110
	Messenger wire suspension longitudinal damping (kNs/m)	1.0
3D catenary	Mass/unit length (kg/m)	0.73
	Bending stiffness (Nm^2)	1100
	Axial stiffness parameter (kN)	17,000
2D catenary	Lumped mass on the contact wire (kg)	0.292

consisting of an equivalent lumped mass approximately reproducing the inertial properties of the steady arm.

As the transition of the catenary is not modelled, at the first and last mast the contact and the messenger wires are fixed also in the longitudinal direction by means of springs and dampers, the longitudinal springs being preloaded in order to apply the proper tension to the wires.

The structural damping of the catenary is introduced according to Rayleigh damping formulation, thus considering directly the proportional damping values as reported in the appendix to the benchmark result paper.

2.2. *Pantograph model*

The pantographs are represented through three-lumped-mass models as defined in the benchmark input data.

2.3. *Model of pantograph–catenary contact*

The contact between the catenary and the pantograph is represented according to the penalty method,[2] defining the normal contact force as a measure of the kinematic constraint violation, both in terms of relative displacement and velocity, between the two bodies. In particular, the interaction is reproduced by a linear contact element, consisting of a spring and a damper in parallel, aimed at minimising the differences in the displacements and in the velocities of the contact point considered as belonging to the collector and to the contact wire, respectively. The contact element is unilateral acting only when the corresponding contact force is higher than zero.

The properties of the contact element, that is, the stiffness and the damping, are chosen in order to keep the frequency response function between the displacements of the contact point considered as belonging to the contact strip and to the contact wire as close to unity as possible in the frequency range of interest, as detailed in [2].

2.4. *Initialisation of the problem (steady-state configuration of the catenary)*

The static configuration of the catenary is defined solving a nonlinear minimisation problem. Overall aim of this process is to derive the catenary geometry and the tension in the contact and messenger wires by prescribing the following input:

- the vertical position of the contact wire at each dropper;
- the average values of the horizontal component of the tensions in the messenger and contact wires;
- the lateral position of the contact wire at the steady arms due to stagger (only for 3D catenaries).

The number of equations is $N = N_d N_c + 2 + (N_c + 1)$, where N_d is the number of droppers in one span and N_c is the span number. The $N_d N_c + 2 + (N_c + 1)$ unknowns of the problem are:

- the length in operation of all droppers ($N_d N_c$ variables);
- the undeformed length of the contact and messenger wire;
- the lateral position of each steady arm hinge ($N_c + 1$ variables).

The problem is solved by means of an iterative procedure (cf. Figure 2), that minimises a residual function constituted by the weighted differences between the actual and the design values of the tensile load in the contact and messenger wires and of the lateral position of the steady arms. Here the expression 'actual values' refers to the values evaluated at the kth iteration of the procedure.

The vertical position of the contact wire at the dropper clamps is otherwise controlled by introducing kinematic constrains, since an accurate solution is required for these quantities. The problem can be therefore formulated as follows:

$$\Delta\ (\mathbf{x}) = \boldsymbol{\delta}(\mathbf{x})^{\mathrm{T}} \mathbf{W} \boldsymbol{\delta}(\mathbf{x}) = \min \quad \text{subject to} : \mathbf{h}(\mathbf{x}) = 0 \tag{1}$$

with $\boldsymbol{\delta}(\mathbf{x})$ the vector of the differences between the current and the design values of the quantities to be minimised, $\mathbf{W}$ a weight matrix, $\mathbf{h}$ the vector collecting the differences between the actual and design values of the contact wire height at the dropper clamps.

To start the minimisation process, an initial guess of the static catenary configuration under the gravity loads is defined using simplified geometrical and static laws and setting to zero the vector $\mathbf{x}$ of minimisation variables (phases 1 and 2 in Figure 2). At each iteration of the

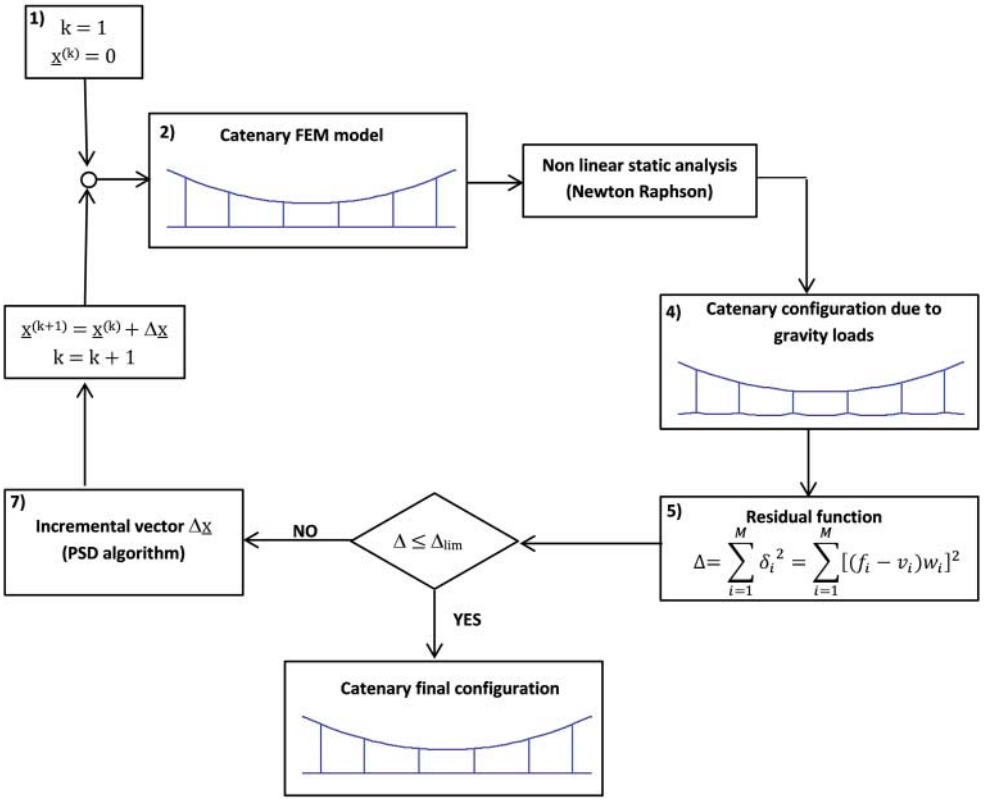

Figure 2. Block diagram of the static procedure.

minimisation procedure, a nonlinear static analysis is performed using the Newton–Raphson method (phase 3) to derive a new static configuration of the catenary (phase 4).

Then, this solution is used to compute the value of the residual function Δ (phase 5). Given a suitable small value Δ_{lim} of the final residual function, if Δ is greater than Δ_{lim}, a new static configuration $\mathbf{x}^{k+1}$ is defined based on the pseudo-second derivative minimisation [3]:

$$\begin{aligned}(\mathbf{A}^{\mathrm{T}}\mathbf{A}+\mathbf{B})(\mathbf{x}^{k+1}-\mathbf{x}^{k})+\mathbf{C}\boldsymbol{\lambda}&=-\mathbf{A}^{\mathrm{T}}\boldsymbol{\delta},\\ \mathbf{C}^{T}(\mathbf{x}^{k+1}-\mathbf{x}^{k})&=-\mathbf{h}(\mathbf{x}^{k}),\end{aligned}\tag{2}$$

where $\boldsymbol{\lambda}$ is a vector of Lagrange multipliers, $\mathbf{A}$ is the first derivative matrix of $\boldsymbol{\delta}$ over $\mathbf{x}$, $\mathbf{C}$ is the first derivative matrix of $\mathbf{h}$ over $\mathbf{x}$, and $\mathbf{B}$ is the matrix accounting for the nonlinear dependence of $\boldsymbol{\delta} = \boldsymbol{\delta}(\mathbf{x})$.

The computation of the first derivative matrix $\mathbf{A}$ is approximated to the incremental ratios following this procedure:

(1) a small increment $\boldsymbol{\Delta}x_{\text{j}}$ is applied to the jth variable and the corresponding catenary is defined according to the same approach described for phase 2;
(2) the static configuration of the catenary under its own weight is calculated through the Newton–Raphson algorithm described at phase 3;
(3) the residual vector $\boldsymbol{\delta}$ is evaluated and the jth column of the first derivative matrix is approximated by the ratios $\boldsymbol{\delta}/\boldsymbol{\Delta}x_{\text{j}}$.

From a theoretical point of view, the elements of matrix **B** are defined according to

$$\boldsymbol{b_{jl}} = \sum_{\boldsymbol{i}=1}^{M} \boldsymbol{\delta_i} \frac{\partial^2 \boldsymbol{\delta_i}}{\partial \boldsymbol{x_j} \partial \boldsymbol{x_l}}, \tag{3}$$

but the computation of the full second derivative matrix based on the same procedure described for the first derivative matrix would require a too high computational effort, and therefore, a simplified approach is followed. The second-order cross derivatives $\partial^2 \boldsymbol{\delta_i} / \partial \boldsymbol{x_j} \partial \boldsymbol{x_l}$ are neglected, while the second-order homogeneous derivatives are approximated by the incremental ratios of the first derivative terms over a step of the iteration loop:

$$b_{jj} = \sum_{i=1}^{M} \delta_i \left. \frac{\partial^2 \delta_i}{\partial {x_j}^2} \right|_{\underline{x}_0} \cong \eta^2 \sum_{i=1}^{M} \delta_i \frac{(\partial \delta_i / \partial x_j)|_{\underline{x}_0}^{k+1} - \partial \delta_i / \partial x_j|_{\underline{x}_0}^{k}}{x_j^{k+1} - x_j^k} . \tag{4}$$

The coefficient η, called damping factor (which is not at all related to the energy dissipated – the name derives from the damping of the numerical solution), has to be conveniently chosen in order to get, for the kth iteration, the best value of the incremental vector $\mathbf{x}^{k+1} - \mathbf{x}^k$, that is, the value leading to the maximum reduction of the residual function Δ according to the boundary conditions imposed by the Lagrange multipliers.

At the end of the static procedure, the static configuration of the catenary is defined, together with the tensile load of the cables and of the steady arms.

2.5. *Numerical integration procedure*

To perform the numerical simulation of dynamic pantograph–catenary interaction, two separate sets of differential equations are written to represent catenary and pantograph dynamics with the contact force exchanged by the contact wire and the pantograph head providing the coupling between the two sets of equations:

$$\begin{aligned} \mathbf{M}_\mathrm{c} \ddot{\mathbf{x}}_\mathrm{c} + \mathbf{C}_\mathrm{c} \dot{\mathbf{x}}_\mathrm{c} + \mathbf{K}_\mathrm{c} \mathbf{x}_\mathrm{c} &= \mathbf{F}_\mathrm{cc}(\mathbf{x}_\mathrm{c}) + \mathbf{F}_\mathrm{cp}(\mathbf{x}_\mathrm{c}, \dot{\mathbf{x}}_\mathrm{c}, \mathbf{x}_\mathrm{p}, \dot{\mathbf{x}}_\mathrm{p}), \\ \mathbf{M}_\mathrm{p} \ddot{\mathbf{x}}_\mathrm{p} + \mathbf{C}_\mathrm{p} \dot{\mathbf{x}}_\mathrm{p} + \mathbf{K}_\mathrm{p} \mathbf{x}_\mathrm{p} &= \mathbf{F}_\mathrm{pc}(\mathbf{x}_\mathrm{c}, \dot{\mathbf{x}}_\mathrm{c}, \mathbf{x}_\mathrm{p}, \dot{\mathbf{x}}_\mathrm{p}). \end{aligned} \tag{5}$$

In the first row of Equation (5), $\mathbf{x}_\mathrm{c}$ and $\mathbf{x}_\mathrm{p}$ are the vectors collecting the catenary nodal displacements and the pantograph coordinates, respectively, $\mathbf{M}_\mathrm{c}$, $\mathbf{C}_\mathrm{c}$ and $\mathbf{K}_\mathrm{c}$ are the mass, damping, and stiffness matrices of the catenary FE model, $\mathbf{F}_\mathrm{cc}$ is the vector of nodal forces accounting for the nonlinear dropper slackening effects, and $\mathbf{F}_\mathrm{cp}$ is the vector containing the generalised nodal forces resulting from the pantograph–catenary contact forces. In the second row of the same equation, $\mathbf{M}_\mathrm{p}$, $\mathbf{C}_\mathrm{p}$, and $\mathbf{K}_\mathrm{p}$ are the pantograph mass, damping, and stiffness matrices and $\mathbf{F}_\mathrm{pc}$ is the vector of the generalised forces acting on the pantograph due to the contact with the catenary. Equation (5) is solved in the time domain using a modified Newmark integration method.[2]

3. Additional methods available

The main additional features of PCaDA can be divided into the following categories:

- special catenary types, including conductor bar catenaries;
- pantograph modelling features;
- prediction of wear in the collector strips and contact wires;
- environmental and operational conditions.

Figure 3. Examples of transitions between sections of conductor bar catenaries (Courtesy of Furrer + Frey).

3.1. *Special catenary types, including conductor bar catenary*

The software allows the modelling of a variety of catenary configurations, including double contact wire and double messenger wire, auxiliary wire for stitched wire suspension, tramway catenaries with delta suspension, and some special arrangements for under bridge zones which include a contact wire height variation to cope with restrictions on the encumbrance.

The software also allows for the simulation of the 'conductor bar catenary' or 'overhead conductor rail', that is, an overhead system featuring an aluminium bar that clamps the contact wire. This is especially adopted in reduced sections tunnel, but due to its advantages in terms of maintenance is becoming more widely used also in ordinary tunnels. The main problem with this catenary type is related to its connection with ordinary conductor line; thus, the model includes also the transition bar between the traditional and conductor bar catenary. The transition bar has a sequence of reductions of the conductor bar section in order to produce a gradual transition from the more deformable traditional catenary and the stiffer conductor bar catenary. The end-section element for the transition between two sections of conductor bar catenary has curved shape in the vertical (and, in case, horizontal) plane (Figure 3).

3.2. *Pantograph modelling features*

The pantograph model available in PCaDA includes several lumped parameter elements, such as rigid bodies, linear and nonlinear springs and viscous dashpots, and friction elements, allowing to model a variety of pantograph designs. A thermodynamic model can be used to model in detail the dynamic behaviour of the air spring acting on the articulated frame; this is mainly used for the investigation of active pantograph control.[4]

PCaDA also allows to consider the deformability of the contact strips using a 'hybrid' pan-tograph model composed by lumped masses and deformable collectors, the latter modelled with a modal superposition approach [5,6] by considering the first deformable modes of the collector. In this way, the frequency range of the model can be significantly increased, pro-vided the mesh of the overhead contact line is refined accordingly and the contact parameters are properly tuned, thereby allowing to study high-frequency interaction problems such as irregular wear of the contacting surfaces (cf. Section 3.3). In [5,6] the frequency range of the model was increased up to 100 Hz by introducing the first two flexural modes of the collector in the model and selecting the upper limit of the range to ensure that the third mode is in quasi-static conditions.

3.3. *Prediction of wear in the collector strips and contact wire*

A special procedure is included in PCaDA, allowing to analyse the formation of wear in the contact strips and in the contact wire.[6] To this aim, the results of the numerical simulation of pantograph–catenary interaction are post-processed according to wear maps taking into account the mechanical factors (contact pressure, friction coefficient, and sliding speed) and the electric factors (electrical resistance at the contact and current flow intensity), these latter being determined according to a model of the electrical contact between the pantograph and the catenary. The wear maps are defined based on laboratory experiments performed on a test rig allowing to perform wear tests on a contact strip/contact wire couple.

3.4. *Environmental and operating condition*

One important issue related to reproducing real operating condition for the pantograph–catenary couple is represented by the contact wire irregularity that can be included as a vertical deviation from the profile calculated after the static initialisation of the problem. The irregularity profile can be derived from experimental measurements performed by a measuring car or can be generated numerically starting from a measured power spectral density function.[7]

The effect of turbulent wind on the pantograph can be accounted for by introducing a time-varying force on each contact strip. The force is defined based on the stochastic properties of the turbulent wind considered and on the drag and lift coefficients of the contact strips derived from wind tunnel tests. Using the same procedure, the forcing effect generated by turbulent wind on the upper and lower pantograph frame can be computed.[8] The effect of side winds acting on the catenary can also be introduced in the simulation, in the form of steady or unsteady nodal forces applied at the nodes of the FE catenary model.

Finally, ice load on the messenger wire can be simulated by properly adjusting the cross-section properties of the wire.

4. Validation of the software

Since the very beginning of PCaDA development, special attention was paid to the validation of the software. In this respect, PCaDA was checked by using the reference model provided by EN50318 standard,[9] the obtained results fulfilling the requirements of the standard as also certified by an independent body.

Moreover, PCaDA results were compared with experimental data coming from line measurements carried out on several pantograph–catenary couples. Different aspects of the pantograph–catenary interaction were considered in the different validation exercises.

In [2], the comparison was performed considering the spectrum of the contact force at 250 km/h and the variation of the statistical maximum and minimum values of the contact force for different speeds. Moreover the capability of the model to correctly reproduce the measured contact wire uplift at midspan in double pantograph operation was verified. The validation was performed considering an ATR95 3 kV pantograph with copper contact strips and the C270 catenary.

The capability of the software to correctly reproduce the interaction with different contact wire tensions was verified in [10], where numerical results were compared to experimental data referring to an ATR95 25 kV pantograph running on 9 tension lengths (10 km approximately) of nominal C270 catenary with 20 kN contact wire tension and 3 upgraded tension

Table 3. Comparison of line measurements and PCaDA simulation results in terms of standard deviation of the contact force, steady arm (SA) uplift, and peak-to-peak displacement of the contact point.

	F_M (N)	σ_F (N)	SA uplift (mm)	z_C peak-to-peak (mm)	σ_F 0–5 Hz (N)	σ_F 8.5–19.5 Hz (N)
Line tests	182.3	47.0	88	47	31.5	28.3
PCaDA	179.3	41.8	77	42	30.1	26.2
Deviation	− 1.6%	− 11.2%	− 12.5%	− 10.6%	− 4.4%	− 7.4%

Note: CX pantograph and LN2 catenary speed 300 km/h.

lengths of C270 catenary with copper–magnesium contact wire tensioned at 30 kN. Not only the overall standard deviation of the contact force and contact point motion were addressed during validation, so as required by EN50318, but also the corresponding rms values divided in the frequency bands related to span passing and to dropper passing, thus enhancing, in the authors' opinion, the confidence in the obtained results.

In [11], the numerical–experimental comparison was aimed at verifying the capability of the software to correctly reproduce the dynamic behaviour associated with the adoption of different pantograph preloads. The interaction between the ATR95 3 kV pantograph equipped with Kasperowski contact strips and the C540 catenary, characterised by double messenger and contact wires, was considered. Also in this case the validation was performed consid-ering the overall standard deviation of the contact force, the contact point motion, and the additional rms values divided in frequency bands, the experimental values being evaluated on several tension lengths. Moreover, the capability of the numerical model in reproducing the pantograph–catenary interaction in multiple (double) pantograph operation was verified by means of comparison between experimental and numerical results for the speed of 250 km/h, considering the same pantograph–catenary couple. The obtained differences on the standard deviation of the contact and on the peak-to-peak displacement of the contact point were lower than 8%, for both leading and trailing pantograph.

At any rate, the deviations of numerical results from measured values were well below the 20% accuracy prescribed by the EN50318 standard [9] in all the reported cases.

PCaDA results were also compared with experimental data referring to pantograph–catenary couples coming from countries other than Italy. With this respect, a comparison between numerical results and experimental data referring to the Swedish couple composed by the WBL pantograph with SSS400 pan-head and the SYT 7.0/9.8 catenary is also reported in [11], in terms of standard deviation and maximum and minimum statistical values of the contact force for different speeds.

Table 3 summarises the results of a validation exercise performed in the framework of PantoTRAIN project, making reference to the French couple [12] formed by the CX pantograph and the LN2 catenary. The validation was performed considering the standard deviation of the contact force in the 0–20 Hz frequency range, the maximum value of the steady arm uplift, and the peak-to-peak displacement of the contact point, as prescribed by EN50318 standard. Moreover, the additional quantities corresponding to the standard deviations of the contact force in the frequency bands interested by span passing (0–5 Hz) and dropper passing (8.5–19.5 Hz) were considered. The measured values were obtained considering eight consecutive section lengths, corresponding to approximately 10 km.

As shown in Table 3, the deviations of simulation results from measured values are all significantly below the 20% accuracy required by EN50318, also when considering the standard deviations divided in frequency. Besides, it is worth mentioning that the simulation with PCaDA was performed considering ideal conditions and in particular the nominal design of the catenary, so that the observed deviations are to be partially ascribed to the differences between the nominal catenary and the actual one.

5. Conclusions

This paper presented the methods for the numerical simulation of pantograph–catenary interaction developed at Politecnico di Milano and implemented in the simulation software PCaDA, providing the details of the catenary, pantograph, and contact model used to produce the results for the benchmark. The paper also provided a description of some advanced features available in the software and aimed at analysing specific issues in pantograph–catenary interaction not addressed in the benchmark.

Comparing results obtained using PCaDA and other simulation codes involved in the benchmark, a very good agreement is generally observed. As far as the static calculation of the catenary is concerned, the benchmark allowed especially to point out the importance of geometric nonlinear effects in the steady arm, affecting significantly the static tension in the droppers and the geometry of the contact wire at the support. The impact of this effect in terms of dynamic simulation results appears, however, to be less significant, although this conclusion needs to be considered as specific for the cases considered in the benchmark, and possibly a larger impact could be found for a different catenary configuration.

Acknowledgements

The authors consider the pantograph–catenary interaction benchmark as a useful initiative that allowed to gain further confidence in the reliability of the simulation techniques available in the field. They would like to thank all the participants in the benchmark for fruitful exchange of ideas and excellent cooperation.

References

[1] Bathe K-J. Finite element procedures in engineering analysis. Englewood Cliffs (NJ): Prentice Hall; 1982.

[2] Collina A, Bruni S. Numerical simulation of pantograph-overhead equipment interaction. Veh Syst Dyn. 2002;38(4):261–291. doi: 10.1076/vesd.38.4.261.8286.

[3] Faggiano A. Automatic lens design with pseudo-second-derivative matrix: a contribution. Appl Opt. 1980;19(24):4226–4229. doi: 10.1364/AO.19.004226.

[4] Carnevale M. Innovative solutions for improving pantograph dynamics and current collection quality [PhD thesis]. Politecnico di Milano; 2010.

[5] Collina A, Lo Conte A, Carnevale M. Effect of collector deformable modes in pantograph–catenary dynamic interaction. Proc Inst Mech Eng F, J Rail Rapid Transit. 2009;223(1):1–14. doi: 10.1243/09544097JRRT212.

[6] Bucca G, Collina A. A procedure for the wear prediction of collector strip and contact wire in pantograph–catenary system. Wear. 2009;266(1–2):46–59. doi: 10.1016/j.wear.2008.05.006.

[7] Collina A, Fossati F, Papi M, Resta F. Impact of overhead line irregularity on current collection and diagnostics based on the measurement of pantograph dynamics. Proc Inst Mech Eng F, J Rail Rapid Transit. 2007;221(4):547–559. doi: 10.1243/09544097F02105.

[8] Pombo J, Ambrósio J, Pereira M, Rauter F, Collina A, Facchinetti A. Influence of the aerodynamic forces on the pantograph–catenary system for high-speed trains. Veh Syst Dyn. 2009;47(11):327–1347. doi: 10.1080/00423110802613402.

[9] European Committee for Electrotechnical Standardization EN 50318. Railway applications – current collection systems – validation of simulation of the dynamic interaction between pantograph and overhead contact line; 2002.

[10] Bruni S, Bucca G, Collina A, Facchinetti A. Numerical and hardware-in-the-loop tools for the design of very high speed pantograph-catenary systems. J Comput Nonlinear Dyn. 2012;7(4). Art. No. 041013, doi: 10.1115/1.4006834.

[11] Bucca G, Carnevale M, Collina A, Facchinetti A, Drugge L, Jönsson P-A, Stichel S. Adoption of different pantographs' preloads to improve multiple collection and speed up existing lines. Veh Syst Dyn. 2012;50(S1):403–418. doi: 10.1080/00423114.2012.665165.

[12] Massat J-P, Laurent C, Nguyen-Tajan TML, Facchinetti A, Bruni S. Simulation tools for virtual homologation of pantographs. Proceedings of the First International Conference on Railway Technology: Research, Development and Maintenance. Stirlingshire, UK: Civil-Comp Press. Paper 70, 2012. doi: 10.4203/ccp.98.70.